International Journal of Mechanical and Materials Engineering (IJMME), Vol. 7 (2012), No. 1, 101–106.

PREDICTION OF FLOW CHARACTERISTICS IN STENOTIC ARTERY USING CIP SCHEME

C.S.N. Azwadi and M. Salehi*
Department of Thermofluids, Faculty of Mechanical Engineering, Universiti Teknologi Malaysia, 81310 UTM Skudai, Johor, Malaysia
*Corresponding author's E-mail: azwadi@fkm.utm.my

Received 01 May 2011, Accepted 30 April 2012

ABSTRACT
This paper presents computational study of blood flow in a stenotic artery using a suitable mathematical model. The artery was modeled as a rigid two-dimensional tube with three different levels of severity of the disease. In the mathematical model, the blood flow equations were governed by the stream function-vorticity equations. Then the cubic interpolation profile scheme with high order of accuracy was applied to discretise the advection term of the equation. Different cases were considered, where the Reynolds number of the blood flow were varied to predict pulsatile of blood flow. The present paper reports the analysis of flow separation area downstream the stenosed artery and the location and peak wall shear stress values. These findings may contribute for early detection and medical treatments to prevent further development of the disease and rupture of the artery.

Keywords: Stenotic Artery, Cubic Interpolation Profile, Stream Function-Vorticity, Advection Equation, Wall Shear Stress.

NOMENCLATURE

u	horizontal flow velocity
v	vertical flow velocity
p	Pressure
D	Diameter of blood capillary
R_0	Radius of blood capillary
u_∞	Inlet flow velocity
ω	Vorticity
ψ	Stream function
ρ	Density of fluid
υ	Viscosity of fluid

1. INTRODUCTION

Heart attack and stroke are the most important causes of death throughout the world. Many people die because of the blood stream constriction in different part of the blood circulation system. Theses constrictions are called atherosclerosis which is created in different parts of the blood circulation system (Ikbal et al., 2011). Because the blood flow behaviour is quite complicated in such regions, it is possible that the stenosis region (a region that blood vessel is occluded partially) would develop and cause more percentage of blood stream blockages. Therefore it is very important to be able to predict these regions before they become clinically dangerous.

According to the experimental investigations on blood vessels, there are special regions that are the most probable for stenosis creation. These regions are blood vessels with bending and bifurcations (Tomaso et al., 2011). In the region of stenosis, there is high wall shear stress which can cause the blood flow separation, recirculation or even turn the flow into turbulent (Ponalagusamy and Tamil, 2011). For example, high shear stress will cause the platelets to be activated and clot the blood flow. This condition is very probable in atherosclerosis disease and basically the main cause of heart attacks (Razavi et al., 2011).

In the past years, many experimental researches have been conducted to investigate the blood flow through stenosis region. Young and Tsai (1973) experimentally studied the laminar steady flow through a rigid tube with 56%, 75% and 89% axisymmetric constriction and concentrated on the pressure and the distribution of wall shear stress. Their works are then extended by Forrester (1970) who considered the effects of the flow separation in an artery with mild stenosis.

Ahmed and Giddens (1983) studied both steady and pulsatile flow through 25%, 50% and 75% constriction of a rigid tube and Reynolds number ranges from 500 to 2000 using laser Doppler anemometry (LDA). Lieber and Giddens (1990) also investigated pulsatile flow through both 75% and 90% constricted rigid tubes. They concentrated their study on the centre line velocity and the wall shear stress distribution before and after the stenosis region. Recently, Shuib et al. (2011) studied the blood flow and the effect of the constriction on the tiny particles passing through different stenosis constriction using particle image velocimetry (PIV) to determine the velocity and the flow image for different constrictions.
The experimental analysis of complex flows, particularly those that are pulsatile and transitional, is both labour-intensive and expensive to perform with great accuracy. Nevertheless, such experimental data is critical for verifying the accuracy of emerging numerical studies of turbulent blood flow.

One of the earliest numerical studies was conducted by Lee and Fung (1970) who simulated the flow through an axisymmetric stenosed rigid tube at low Reynolds numbers ($0 < Re < 25$). As the computers improved and became capable of dealing with more complicated geometries, more complicated models were solved; for

example, Wille (1980) and Rindt et al. (1987), who studied the flow through two-dimensional bifurcation models at wide range of Reynolds numbers.

In order to analyze the structure of secondary flows for biomedical purposes, Perktold et al. (1991) performed three-dimensional simulations of pulsatile flow in carotid bifurcation artery. Perktold and Rappitsch (1995) then extended this work by considering distensible walls to resemble the blood capillary. They reported that in the distensible walls model, the wall shear stress decreases and the recirculation and separation regions are slightly reduced in size. However, the general behaviour of the flow is the same as the rigid wall model.

In order to provide more accurate and realistic simulation of blood flow in arteries, Smith et al. (1996) provided an idealized physiologically relevant stenosed carotid bifurcation model. In their simulation, they tried to design a geometry which is adapted to the real shape of a stenosed artery in a bifurcation. These works were then extended by Steinman (2002), Steinman et al. (2000) and Gin et al. (2002).

Recently many researchers are trying to add more sophisticated details to the blood stream simulation, like assuming the elasticity and pulsation behaviour of the blood vessels (Cho et al., 2011), or simulating flow as a non-Newtonian fluid (Prashanta, 2005 and Ikbal et al., 2011).Since a stenotic artery may have different sizes and complex flow structure at the downstream region, an attempt is made develop a high accurate numerical model with low computational cost to explore the characteristic of Newtonian typed of blood flow through axisymmetrical straight diseased artery. Additionally, comparisons of different data mentioned above show a scatter result for the behavior of blood flow especially the dependence of reattachment length on Reynolds numbers and the magnitude and location of maximum shear stress on the stenotic body.

Therefore, other than to improve our understanding on stenotic flow in axisymmetrical diseased artery with variant degrees of stenosis, more importantly, one of the objectives of the present investigation is to demonstrate an alternative finite different scheme that can be employed to predict the blood flow behavior at high accuracy and low computational time.

2. PROBLEM FORMULATIONS

In present study, the governing equation of two-dimensional, incompressible and isothermal fluid flow is considered. Therefore, the governing continuity and x- and y-momentum equations can be expressed as follow (Hasanuzzaman et al., 2007)

$$\frac{\partial u}{\partial x}+\frac{\partial v}{\partial y}=0 \tag{1}$$

$$\frac{\partial u}{\partial t}+u\frac{\partial u}{\partial x}+v\frac{\partial u}{\partial y}=-\frac{1}{\rho}\frac{\partial p}{\partial x}+\upsilon\left(\frac{\partial^2 u}{\partial x^2}+\frac{\partial^2 u}{\partial y^2}\right) \tag{2}$$

$$\frac{\partial v}{\partial t}+u\frac{\partial v}{\partial x}+v\frac{\partial v}{\partial y}=-\frac{1}{\rho}\frac{\partial p}{\partial y}+\upsilon\left(\frac{\partial^2 v}{\partial x^2}+\frac{\partial^2 v}{\partial y^2}\right) \tag{3}$$

In this work, the pressure term in the Eqs. (2) and (3) are eliminated and rewrite in terms of vorticity function as follow (Azwadi and Idris, 2010)

$$\frac{\partial \omega}{\partial t}+u\frac{\partial \omega}{\partial x}+v\frac{\partial \omega}{\partial y}=\upsilon\left(\frac{\partial^2 \omega}{\partial x^2}+\frac{\partial^2 \omega}{\partial y^2}\right) \tag{4}$$

In terms of stream function, the equation defining the vorticity becomes

$$\omega=-\left(\frac{\partial^2 \psi}{\partial x^2}+\frac{\partial^2 \psi}{\partial y^2}\right) \tag{5}$$

Before considering any numerical solution to the above set of equations, it is convenient to rewrite the equations in terms of dimensionless variables. The following dimensionless variables will be used here

$$\begin{aligned}&\Psi=\frac{\psi}{u_\infty D},\Omega=\frac{\omega H^2\,\mathrm{Pr}}{\upsilon}\\&U=\frac{u}{u_\infty},V=\frac{v}{u_\infty}\\&X=\frac{x}{D},Y=\frac{y}{D},T=\frac{tu_\infty}{D}\end{aligned} \tag{6}$$

In terms of these variables, Eqs. (4) and (5) become

$$\frac{\partial \Omega}{\partial T}+U\frac{\partial \Omega}{\partial X}+V\frac{\partial \Omega}{\partial Y}=\frac{1}{\mathrm{Re}}\left(\frac{\partial^2 \Omega}{\partial X^2}+\frac{\partial^2 \Omega}{\partial Y^2}\right) \tag{7}$$

$$\Omega=-\left(\frac{\partial^2 \Psi}{\partial X^2}+\frac{\partial^2 \Psi}{\partial Y^2}\right) \tag{8}$$

where the dimensionless parameter Reynolds number, Re is defined as

$$\mathrm{Re}=\frac{u_\infty D}{\upsilon} \tag{9}$$

In the present study, we bring the so-called Cubic interpolated profile method (CIP) (Takewaki et al., 1985 and Azwadi and Attarzadeh, 2011) to solve the hyperbolic type of the governing equations. The CIP is known as a numerical method for solving the advection term with low numerical diffusion. This method constructs a solution inside the grid cell close enough to the real solution of the given equation (Nakamura and Yabe, 1999 and Azwadi and Rahman, 2009).

To see this, we begin by recalling Eq. (7) and its spatial derivatives, and split them into advection and nonadvection phases as follow
Advection phase:

$$\frac{\partial \Omega}{\partial \tau} = -\left(U \frac{\partial \Omega}{\partial X} + V \frac{\partial \Omega}{\partial Y} \right) \tag{10}$$

$$\frac{\partial \Omega_x}{\partial \tau} = -\left(U \frac{\partial \Omega_x}{\partial X} + V \frac{\partial \Omega_x}{\partial Y} \right) \tag{11}$$

$$\frac{\partial \Omega_y}{\partial \tau} = -\left(\frac{U}{\varepsilon} \frac{\partial \Omega_y}{\partial X} + \frac{V}{\varepsilon} \frac{\partial \Omega_y}{\partial Y} \right) \tag{12}$$

Nonadvection phase:

$$\frac{\partial \Omega}{\partial \tau} = \frac{1}{Re}\left(\frac{\partial^2 \Omega}{\partial X^2} + \frac{\partial^2 \Omega}{\partial Y^2} \right) \tag{13}$$

$$\frac{\partial \Omega_x}{\partial \tau} = \frac{1}{\mathrm{Re}}\left(\frac{\partial^3 \Omega}{\partial X^3} + \frac{\partial^3 \Omega}{\partial X \partial Y^2} \right) - \frac{\partial U}{\partial X}\frac{\partial \Omega}{\partial X} - \frac{\partial V}{\partial X}\frac{\partial \Omega}{\partial Y} \tag{14}$$

$$\frac{\partial \Omega_y}{\partial \tau} = \frac{1}{Re}\left(\frac{\partial^3 \Omega}{\partial X^2 \partial Y} + \frac{\partial^3 \Omega}{\partial Y^3} \right) - \frac{\partial U}{\partial Y}\frac{\partial \Omega}{\partial X} - \frac{\partial V}{\partial Y}\frac{\partial \Omega}{\partial Y} \tag{15}$$

where $\Omega_x = \partial \Omega / \partial x$ and $\Omega_y = \partial \Omega / \partial y$.
In the proposed method, the advection phase of the spatial quantities in the grid interval are approximated with constrained polynomial using the value the it's spatial derivative at neighbouring grid points as follow

$$F_{i,j}(X,Y) = \left[\left(a_1 \tilde{X} + a_2 \tilde{X} + a_3\right)\tilde{X} + a_4 \tilde{Y} + \Omega_x\right]\tilde{X} + \left[\left(a_5 \tilde{Y} + a_6 \tilde{X} + a_7\right)\tilde{Y} + \Omega_y\right]\tilde{Y} + \Omega \tag{16}$$

where $\tilde{X} = X - X_{i,j}$ and $\tilde{Y} = Y - Y_{i,j}$. The coefficients of a_1, $a_2, \ldots a_7$ are determined so that the interpolation function and its first derivatives are continuous at both ends.
restriction, the numerical diffusion can be greatly reduced when the interpolated profile is constructed. The spatial derivatives are then calculated as

$$F_{x,i,j}(X,Y) = \left(3a_1 \tilde{X} + 2a_2 \tilde{Y} + a_3\right)\tilde{X} + \left(a_4 + a_6 \tilde{Y}\right)\tilde{Y} + \Omega_x \tag{17}$$

$$F_{y,i,j}(X,Y) = \left(2a_2 \tilde{Y} + a_3\right)\tilde{X} + \left(3a_5 \tilde{Y} + 2a_6 \tilde{X} + 2a_7\right)\tilde{Y} + \Omega_y \tag{18}$$

In two-dimensional case, the advected profile is approximated as follow

$$\Omega^n_{i,j} = F_{i,j}(X + \eta, Y + \xi) \tag{19}$$

$$\Omega^n_{x,i,j} = F_{x,i,j}(X + \eta, Y + \xi) \tag{20}$$

$$\Omega^n_{y,i,j} = F_{y,i,j}(X + \eta, Y + \xi) \tag{21}$$

where $\eta = -U\Delta\tau$ and $\xi = -V\Delta\tau$.

The newly calculated spatial quantities are then be used to solve non-advection phase of Eqns. (13) to (15) and vorticity formulation of Eq. (8). In present study, the explicit central finite different discretisation method is applied with second order accuracy in space. For example, the treatment for Eq. (8) is

$$\Psi^n_{i,j} = \frac{\dfrac{\Psi^n_{i+1,j} + \Psi^n_{i-1,j}}{(\Delta X)^2} + \dfrac{\Psi^n_{i,j+1} + \Psi^n_{i,j-1} + \Omega^n_{i,j}}{(\Delta X)^2}}{\dfrac{2}{(\Delta X)^2} + \dfrac{2}{(\Delta Y)^2}} \tag{22}$$

3. PROBLEM PHYSICS

A schematic of the stenosed artery with rigid walls considered in this research is shown in Figure1. as in Young and Tsai (1973).

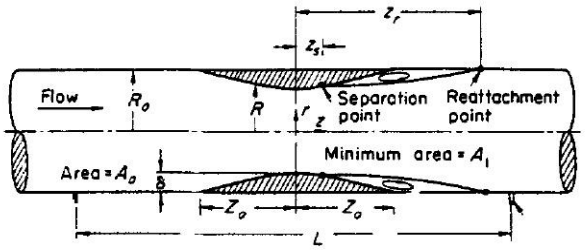

Figure 1 Geometry of the stenotic artery (Young and Tsai, 1973).

The geometry is two-dimensional axisymmetric tube with rigid walls. The shape of the constricted region is important and it is specified like a cosine curve as follow

$$\frac{R}{R_0} = 1 - \frac{\delta}{2R_0}\left(1 + \cos\frac{\pi z}{Z_0}\right) \tag{23}$$

for $-Z \le z \le Z_0$. It is important to mention that there are many more geometrical shapes that are defined by different researchers. Some of them assume the constriction region as a parabolic equation but due most of the studies use the cosine curve, this shape was chosen as reference. The inlet and outlet flows are considered fully developed. Therefore an outlet length was set long enough to ensure that the outlet boundary conditions did not influence the flow in the vicinity of the stenosis.
Basically there are two types of stenosis subjected to their Z_0/R_0 ratio. The stenoses with $Z_0/R_0 = 4$ is considered as mild stenosis while for $Z_0/R_0 = 2$ is a severe stenosis. In the present research, the characteristics of blood flow through three types of severe stenosis at three different constriction percentages were investigated as in Table 1.

Table 1 Three types of severe stenosis at three different constriction percentages

Model No	$R_0\,(cm)$	δ	Z_0/R_0	Percentage of Stenoses
M-1	1	0.34	2	56%
M-2	1	0.50	2	75%
M-3	1	0.67	2	89%

4. NUMERICAL RESULTS

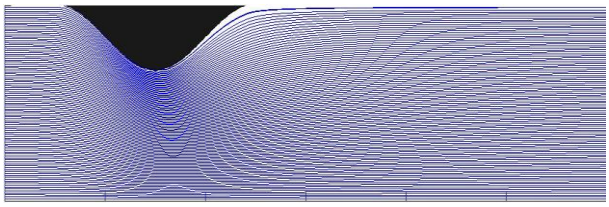

Figure 2(a) Streamlines contour at constriction of 56% and Re = 100

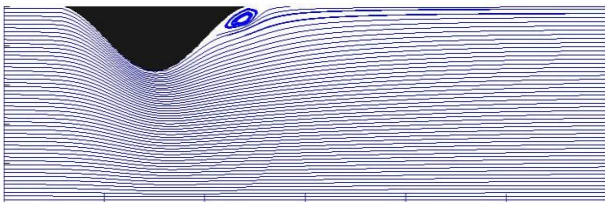

Figure 2(b) Streamlines contour at constriction of 56% and Re = 200

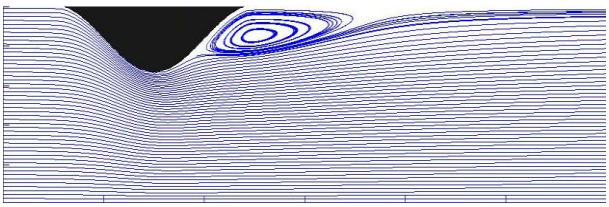

Figure 2(c) Streamlines contour at constriction of 56% and Re = 600

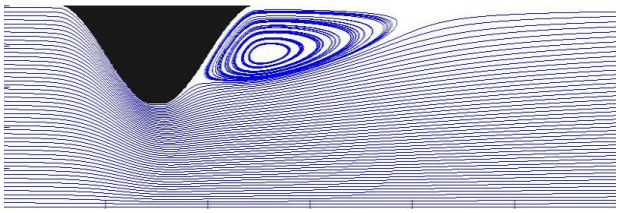

Figure 3(b) Streamlines contour at contriction of 75% and *Re* = 200

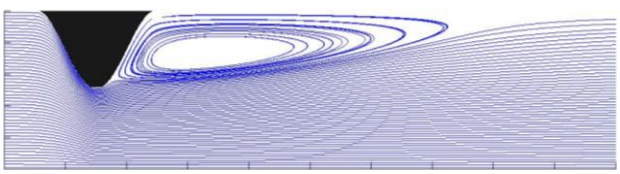

Figure 3(c) Streamlines contour at contriction of 75% and *Re* = 600

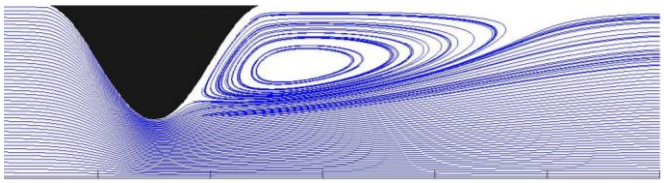

Figure 4(a) Streamlines contour at contriction of 89% and *Re* = 100

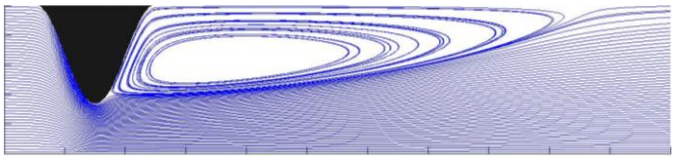

Figure 4(b) Streamlines contour at contriction of 89% and *Re* = 200

Figures 2-4 show plots of streamline contours for respective conditions. These figures clearly exhibit the formation of recirculation region downstream of the stenotic artery for most of the cases. They can be seen that an artery with a more severe stenosis, the flow recirculation region was larger and its strength was also increase. However, no recirculation region was present for 56% percentage of stenosis and Reynolds number of 100. Our simulated results also indicated that there is no steady solution for the most severe stenoses (89%) and Reynolds number 600. These findings agree well with the results obtained by Young and Tsai (1973).

The separation point and recirculation length for the considered Reynolds number were then determined and tabulated in Table 2. The table clearly indicates the significant effect of the stenosis geometry and the Reynolds number on the size of recirculation region.

Table 2 Separation point and reattachment length of flow through stenosed artery

% of Constriction	Re = 100		Re = 200		Re = 600	
	SP	RL	SP	RL	SP	RL
56%	--	--	4.19	5.22	3.81	7.73
75%	3.90	6.25	3.74	8.47	3.52	16.76
89%	3.60	10.26	3.51	16.52	--	--

Note: SP (Separation point), RL (Reattachment length)

The wall shear stress is one of the most important parameters in the initiation of atherosclerosis. In the present study, the wall shear stress has been computed by the following equation

$$\tau = \mu \frac{\partial U}{\partial Y} \tag{24}$$

Figure 5 illustrates the shear stress variation along the solid surface at a respective constriction and different Reynolds number. They can be seen that the magnitude of wall shear stress increase rapidly when the flow

approaches the neck of stenosis. It then decreases to the minimum point before it recovers gradually in the downstream of the stenosis. The location of zero shear stress indicates the separation and reattachment of the developed vortices. Therefore, negative values of shear stress demonstrate the presence of recirculation region of the blood flow. It is noted that for the case of 56% of constriction, no separation of flow occurs at Re = 100.

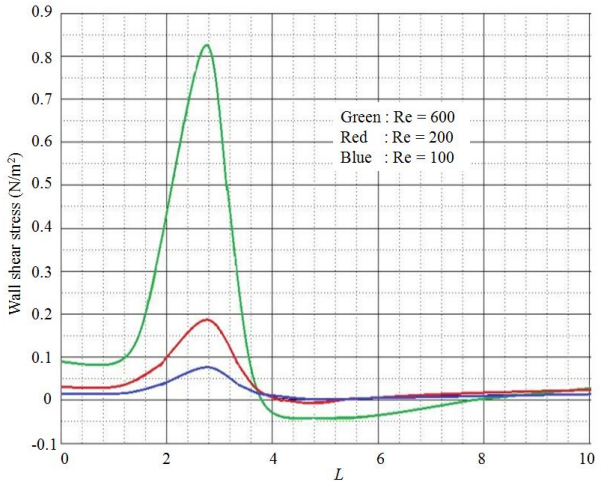

Figure 5a Distribution of wall shear stress for 56% of constriction

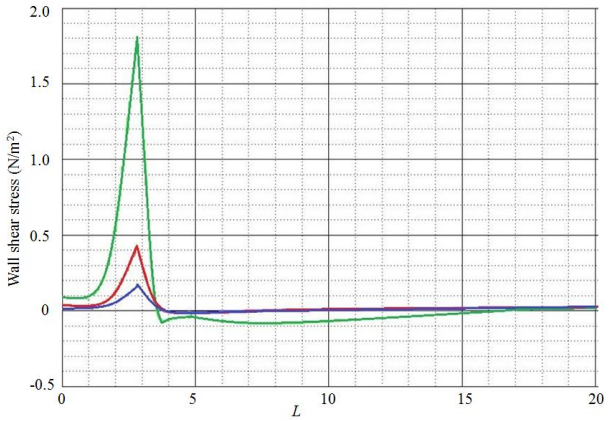

Figure 5b Distribution of wall shear stress for 75% of constriction

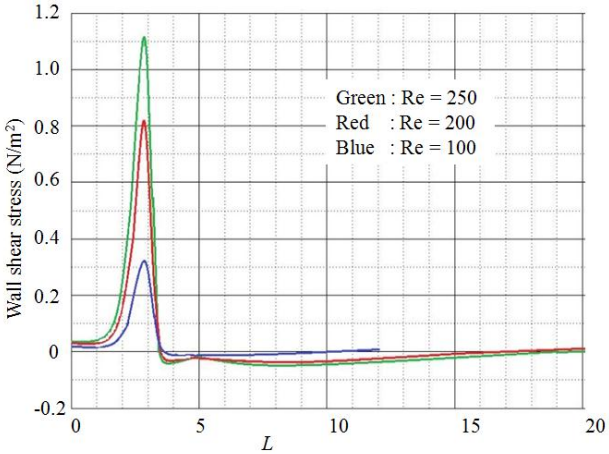

Figure 5c Distribution of wall shear stress for 89% of constriction

For higher values of Reynolds numbers, the region of negative value of wall shear stress getting longer and longer indicates bigger and bigger size of vortex downstream the stenosis. This may results in further development of atherosclerotic plaque and expansion of stenosis area. Similar patterns can be observed for two other levels of severities. They demonstrate that as the Reynolds number increase, the location of peak shear stress shift slightly downstream as shown in Table 3.

Table 3 location and values of peak shear stress

% of Constriction	Re = 100		Re = 200		Re = 600	
	LST	ST	LST	ST	LST	ST
56%	2.78	0.077	2.78	0.189	2.78	0.827
75%	2.82	0.177	2.82	0.4354	2.82	1.815
89%	2.84	0.324	2.84	0.821	--	--

Note: LST (Location of peak shear stress), ST (Value of peak shear stress)

5. CONCLUSION

Blood flow in a stenotic artery has been investigated numerically using the cubic interpolation profile method. The results of flow variables such as shear stress distribution and recirculation flow have been computed for different level of severity of the disease and wide range of Reynolds numbers. The development of negative wall shear stress downstream the stenosis is found to be the prime development of further atheroclerosis plaque and expansion of stenosis area. The results have demonstrated that they are quite encouraging and in good agreement with the previously published data. It is hoped that these findings could be used in for early detection and medical treatments to prevent further development of the disease and rupture of the artery.

REFERENCES

Ahmed, S.A. and Giddens, D.P. 1983. Velocity measurements in steady flow through axisymmetric stenoses at moderate Reynolds numbers, Journal of Biomechanics 16 (7): 505-507.

Azwadi C.S.N. and Attarzadeh S.M. 2011. An accurate numerical prediction of solid particle fluid flow in a lid-driven cavity, International Journal of Mechanics 5 (3): 123-128.

Azwadi C.S.N. and Rahman M.R.A. 2009. Cubic interpolated pseudo particle (CIP)-thermal BGK lattice Boltzmann numerical scheme for solving incompressible thermal fluid flow problem, Malaysian Journal of Mathematical Science 3(2): 183-202.

Azwadi, C.S.N. and Idris, M.S. 2010. Finite different and lattice Botlzmann modeling for simulation of natural convection in a square cavity, International Journal of Mechanical and Materials Engineering 5 (1): 80-86.

Cho, S.W., Kim, S.W., Sung, M.H., Ro, K.C. and Ryou, H.S. 2011. Fluid-structure interaction analysis on the effects of vessel arterial properties on blood flow characteristics in stenosed arteries under axial rotation, Korea-Australia Rheology Journal 23 (1): 7-16.

Forrester, J.H. 1970. Flow through a converging-diverging tube and its application in occlusive vascular disease, Journal of Biomechanics 3 (3): 297-306.

Gin, R., Straatman, A.G. and Steinman, D.A. 2002. A dual-pressure boundary condition for use in simulations of bifurcating conduits, Journal of Biomechanical Engineering 124 (5): 617-619.

Hasanuzzaman, M., Saidur, R., Ali., Masjuki, H.H. 2007. Effects of variables on natural convection heat transfer through V-corrugated vertical plates, International Journal of Mechanical and Materials Engineering 2 (2): 109-117.

Ikbal, M.A., Chakravarty, S., Sarifuddin and Mandal, P.K. 2011. Numerical simulation of mass transfer to micropolar fluid flow past a stenosed artery, International Journal for Numerical Methods in Fluids 67 (11): 1655–1676.

Lee, J.S. and Fung, Y.C. 1970. Flow in locally constricted tubes at low Reynolds numbers, Journal of Applied Mechanics 37 (1): 9-16.

Lieber, B.B. and Giddens, D.P. 1990. Post-stenotic core flow behavior in pulsatile flow and its effects on wall shear stress, Journal of Biomechanics 23 (6): 597-605.

Nakamura, T. and Yabe, T. 1999. Cubic interpolated propagation scheme for solving the hyper dimensional Vlasov-Poisson equation in phase space, Computer Physics Communication 120 (2): 122-154.

Perktold, K. and Rappitsch, G. 1995. Computer simulation of local blood flow and vessel mechanics in a compliant carotid artery bifurcation model, Journal of Biomechanics 28 (7): 845-856.

Perktold, K., Resch, M. and Peter, R.O. 1991. Three-dimensional numerical analysis of pulsatile flow and wall shear stress in the carotid artery bifurcation, Journal of Biomechanics 24 (6): 409-420.

Ponalagusamy, R. and Tamil, S.R. 2011. A study on two-layered model (Casson-Newtonian) for blood flow through an arterial stenosis: Axially variable slip velocity at the wall, Journal of the Franklin Institute-Engineering and Applied Mathematics 348 (1): 2308-2321.

Prashanta, K.M. 2005. An unsteady analysis of Non-Newtotian blood flow through tapered arteries with stenosis, International Journal of Non-Linear Mechanics 40 (1): 151-164.

Razavi, A., Shirani, E. and Sadeghi, M.R. 2011. Numerical simulation of blood pulsatile flow in a stenosed carotid artery using different rheological models, Journal of Biomechanics 44 (11): 2021-2030.

Rindt, C.C.M., Vosse, F.N.V.D., Steenhoven, A.A.V., Janssen, J.D. and Reneman, R.S. 1987. A numerical and experimental analysis of the flow field in a two-dimensional model of the human carotid artery bifurcation, Journal of Biomechanics 20 (5): 499-509.

Shuib, A., Hoskins, P. and Easson, W. 2011. Experimental investigation of particle distribution in a flow through a stenosed artery, Journal of Mechanical Science and Technology 25 (2): 357-364.

Smith, R.F., Rutt, B.K., Fox, A.J. and Rankin, R.N. 1996. Geometric characterization of stenosed human carotid arteries, Academic radiology 3 (11): 898-911.

Steinman, D.A. 2002. Image-based computational fluid dynamics modeling in realistic arterial geometries, Annals of Biomedical Engineering 30 (1): 483-497.

Steinman, D.A., Poepping, T.L., Tambasco, M., Rankin, R.N. and Holdsworth, D.W. 2000. Flow patterns at the stenosed carotid bifurcation: effect of concentric versus eccentric stenosis, Annals of Biomedical Engineering 28 (4): 415-423.

Takewaki, H., Nishigushi, A. and Yabe, T. 1985. Cubic interpolated pseudo particle method for solving hyperbolic type equations, Journal of Computational Physics 61(2): 261-268.

Tomaso, D., Giulia., Diaz-Zuccarini., Vanessa. and Pichardo-Almarza, C. 2011. A Multiscale Model of Atherosclerotic Plaque Formation at Its Early Stage, Biomedical Engineering, IEEE Transactions 58 (12): 3460-3463.

Wille, S.O. 1980. Pressure and flow in two dimensional numerical bifurcation models, Applied Mathematical Modeling 4 (1): 351-356.

Young, D.F. and Tsai, F.Y. 1973. Flow characteristics in models of arterial stenoses -- I. Steady flow, Journal of Biomechanics 6 (4): 395-402.